Volume 8, Number 6 (December 2015) p. 827-859 • ISSN 1983-4195
http://dx.doi.org/10.1590/S1983-41952015000600006

REVISTA IBRACON DE ESTRUTURAS E MATERIAIS
IBRACON STRUCTURES AND MATERIALS JOURNAL

Study of methods for the design of cellular composite steel and concrete beams

Estudo de metodologias para o dimensionamento de vigas mistas de aço e concreto com perfil celular

A. BADKE-NETO [a]
augbadke@gmail.com

A. F. G. CALENZANI [a]
afcalenzani@gmail.com

W. G. FERREIRA [a]
walnorio@gmail.com

Abstract

Currently, with the advancement of welding and cutting technology, steel profiles with circular openings, called cellular profiles, have become widely used as beams. The ABNT NBR 8800:2008 and international standards do not address cellular steel beams and cellular composite steel and concrete beams, which contributes to their limited use. A computer program was developed and validated for the design of cellular composite steel and concrete simply supported beams based on two different methods from the literature. The use of this computational tool made possible a parametric study comprising cellular composite beams obtained from two different rolled steel I sections. In this study, the influence of the geometric parameters of the cellular profile and the influence of beam span in the strength and in the failure mode was analyzed. It was concluded that in many situations the use of composite cellular beams is advantageous in relation to original composite beams.

Keywords: cellular composite steel and concrete beams, cellular beams, design.

Resumo

Atualmente, com o avanço da tecnologia de corte e solda, perfis de aço com aberturas sequenciais na forma circular, denominados perfis celulares, vêm sendo bastante utilizadas como vigas de edificações. A ABNT NBR 8800:2008 e as normas estrangeiras não abordam vigas de aço e vigas mistas de aço e concreto com perfil celular, o que contribui para que o seu uso seja limitado. Foi desenvolvido e aferido um programa computacional para o dimensionamento de vigas mistas de aço e concreto com perfil celular biapoiadas de acordo com duas metodologias distintas da literatura. Um estudo paramétrico abordando vigas mistas com perfis celulares obtidos de dois perfis I de aço laminados comerciais foi realizado. Nesse estudo, a influência dos parâmetros geométricos do perfil celular e do comprimento do vão da viga na resistência e na forma de colapso foi analisada. Foi possível concluir que em muitas situações o uso de vigas mistas com perfil celular é vantajoso em relação às vigas mistas de alma cheia.

Palavras-chave: vigas mistas de aço e concreto com perfis celulares, vigas alveolares, dimensionamento.

[a] *Centro Tecnológico, Universidade Federal do Espírito Santo, Vitória, ES, Brasil.*

Received: 02 Jun 2015 • Accepted: 18 Sep 2015 • Available Online: 24 Nov 2015

1. Introduction

1.1 Generalities

The steel beams with sequential openings in the web were created from structural requirements of weight reduction and are manufactured from rolled profiles, with standardized openings in the web. These beams are also referred to in the technical literature as "expanded web beams". The openings in the web can be fabricated in the form of hexagons or circles, resulting respectively in castellated or cellular beams, Figure 1.

Figure 1 – Steel beams with sequential openings in the web

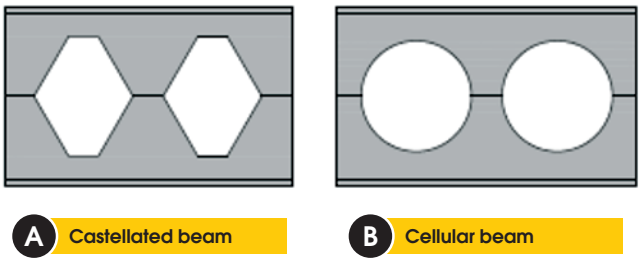

Cellular beams are made from I or H sections, whose web is cut longitudinally in the desired format. Then, the two halves are displaced and welded by the axis, in order to generate openings in sequence along the web and increase in height of the cross section, Figure 2.

The search for a rational use of resources in the design of structural steel buildings often induces the choice of solutions that facilitate the integration of services with the structure. Accordingly, the design of steel beams with web openings for the passage of service ducts have been increasingly demanded. Cellular beams are quite used as they allow the passage of ducts through the openings, by integrating the facilities with the floor system, reducing the vertical space required per floor.

The cellular beam has represented a highly competitive solution. One of its great advantages is that with virtually the same amount of steel as the original beam, a much higher moment strength can be achieved, due the increased height of the cross section, making it possible to overcome longer spans, which will reduce the numbers of columns resulting in a lower cost and greater speed of erection. Even from an economic point of view, manufacturing operations have relatively little cost, and are compensated by increased load capacity and stiffness.

In contrast to the advantages, the beams have reduced capacity to shear, which may require reinforcement of the web, generating significant cost. They are still inefficient in resisting the stresses resulting from localized forces, being more suitable for large spans subjected to small loads.

Cellular beams can be designed as composite when there is a shear connection between the steel and the concrete slab, thus being able to overcome even greater spans than the conventional composite beam, due to the increased stiffness provided by the geometry of the cellular beam.

Cellular beams are not used to their full potential for not being included in the national steel structure design standard, ABNT NBR 8800: 2008 [2] and also because they are unknown to most designers.

This paper aims at the development of a computer program with the methods of Ward [3] and Lawson and Hicks [4] for the design of cellular composite steel and concrete beams, to analyze the influence of the cellular beam geometry on the ultimate load and failure mode of a series of cellular composite beams, constituted from the connection between the cellular steel profile and the composite slab. Additionally, the results obtained from the computer program for each method are compared with each other and with experimental results from the literature.

1.2 Failure modes

1.2.1 Formation of Vierendeel mechanism

The presence of shear forces of high magnitudes on the beam implies the formation of the Vierendeel mechanism (Figure 3 (a)). The formation of plastic hinges occurs at the corners of the openings, deforming the beam in the manner of a parallelogram-. This mechanism is more likely to develop in the beams with short spans, shallow tee-section and long weld between two openings.

Figure 2 – Fabrication of cellular beams (1)

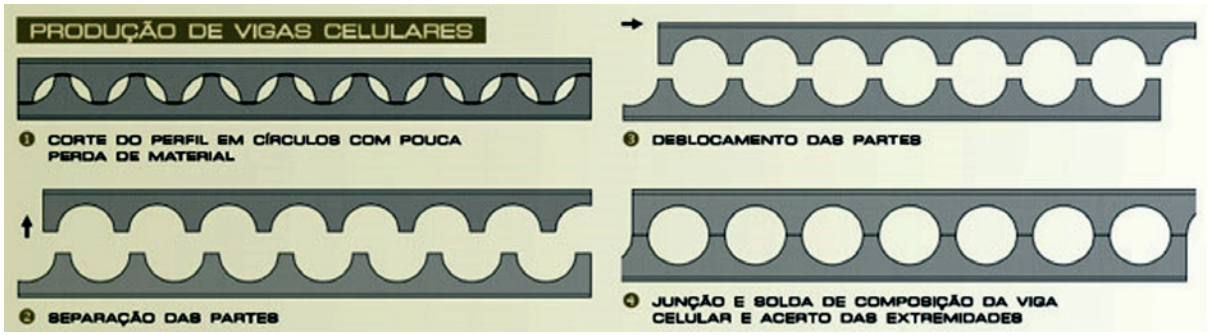

Figure 3 – Failure modes (5)

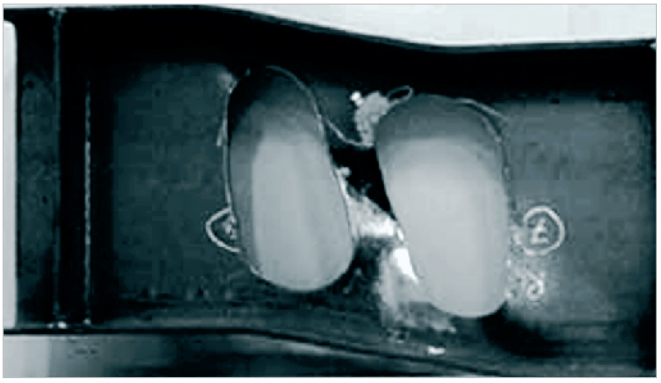

A Vierendeel mechanism

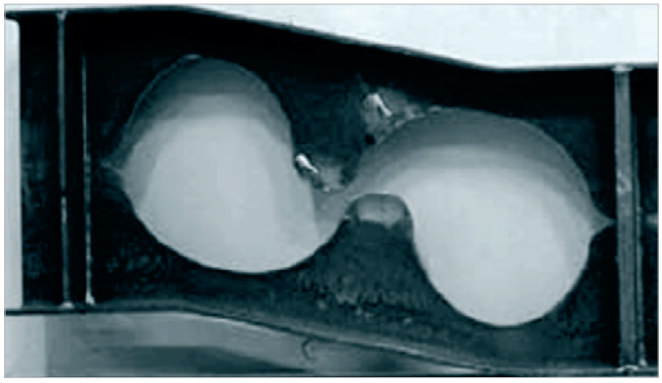

B Rupture of the welded joint in a web post

The failure will occur at the opening with the maximum shear force. In the case of openings with the same shear force, this failure will occur at the opening with the greatest bending moment.

1.2.2 Formation of plastic hinges

This failure occurs when the bending moment makes the upper and lower tees yield by tension and compression. The moment strength is equal to the plastic moment of a section taken through the vertical centerline of an opening.

1,2,3 Rupture of the welded joint

The rupture of the welded joint occurs when the longitudinal shear stress exceeds the weld resistance (Figure 3 (b)). This failure mode depends on the spacing of openings. There will be a greater chance of failure for smaller openings spacing.

1.2.4 Lateral torsional buckling

The lateral torsional buckling is characterized by a lateral displacement and a rotation of the cross section. According to Kerdal and Nethercot [6], the cellular beams and solid web beams have similar behaviors with regard to lateral buckling, but the geometric properties of cellular beams should be taken in the centerline of the openings.

1.2.5 Web post buckling due to shear

The shear force V_{WP} (Figure 4), acting along the welded joint stress

Figure 4 – Web post buckling due to shear (7)

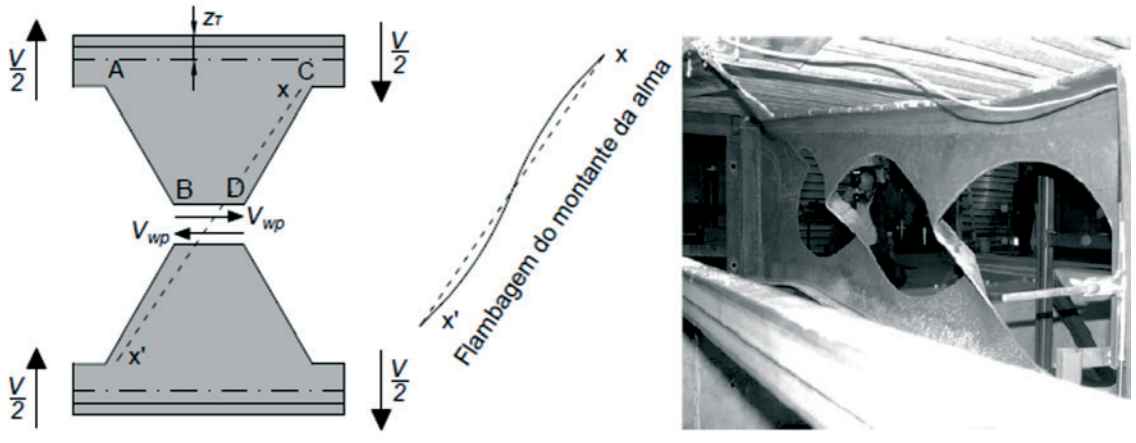

the web post in bending, causing tensile stress on contour AB and compression on the contour CD. In the web post buckling due to shear the compressed part tends to move away from the longitudinal plane of the section while the tensioned part tends to remain in the starting position. According to Kerdal and Nethercot [6], this failure mode normally occurs in inelastic regime with a significant yielding of the sections.

1.2.6 Web post buckling due to compression

Web post buckling due to compression occurs by the presence of localized loads or support reactions directly applied in the web post. It is similar to - buckling of axially compressed bars.

1.3 Methodologies for the design of cellular composite steel and concrete beams

In this research were used two methods for the design of cellular composite steel and concrete beams, extracted from Ward [3] and Lawson and Hicks [4] design guides. Both design guides use the prescriptions of European standards when referring to limit states and design resistances already established. The formulations of the cited methods were adapted to meet the criteria of the ABNT NBR 8800: 2008. Items 1.3.1 and 1.3.2 briefly describe the design strength for each ultimate limit state approached by these methods.

1.3.1 Lawson e Hicks [4] method

1.3.1.1 Shear strength at an opening

The shear strength of a cellular composite beam is established as the shear strength of the steel section plus the shear strength of the concrete slab. The shear plastic strength of the steel section at the opening is equal to:

$$V_{pl,Rd} = \frac{0.6 A_w f_y}{\gamma_{a1}} \quad (1)$$

where A_w is the sum of the areas of the upper and lower tee webs, f_y is the yield strength of steel and γ_{a1} is the resistance factor of steel cross sections, equal to 1.10.
For composite steel and concrete slabs, the shear force strength per unit length must be obtained according to the ABNT NBR 8800: 2008 [2]. For solid reinforced concrete slabs, the ABNT NBR 6118: 2014 [8] is used for the calculation of this shear strength. In both cases, the value of the shear force strength per unit length is multiplied by an effective width, b_w, given by $b_w = b_f + 2h_{t,ef}$, where b_f is the flange width of the steel section and $h_{t,ef}$ is the effective depth of the slab. Regardless of the use of steel deck, the effective depth of the slab can be considered as 75% of its total depth ($0.75h_t$).

1.3.1.2 Moment strength at an opening

There are two different situations to determinate the plastic moment strength. In the first case it is assumed that the plastic neutral axis is in the slab, while in the second its location is admitted in the top tee of the steel section. When the plastic neutral axis is in the slab, the moment strength is given by:

$$M_{o,Rd} = N_{bT,Rd}\left(h_{ef} + z_T + h_t - \frac{1}{2} z_c\right) \quad (2)$$

When the plastic neutral axis is in the top tee of the steel section, the moment strength is defined as:

$$M_{o,Rd} = N_{bT,Rd} h_{ef} + N_{c,Rd}\left(z_T + h_t - \frac{1}{2} t_c\right) \quad (3)$$

where $N_{bT,Rd}$ is the axial force in the bottom tee, h_{ef} is the effective depth of the beam between the centroids of the tees, h_t is the slab depth, z_T is the depth of the centroid of the top tee from the outer edge of the flange, z_c is the depth of concrete in compression e $N_{c,Rd}$ is the compression strength of the concrete slab.

1.3.1.3 Vierendeel mechanism

The Vierendeel moment strength is the sum of the Vierendeel moment strengths at the four corners of the opening, with the contribution due to local composite action between the top tee and the slab. The Vierendeel moment strength must be greater than the design value of the difference in bending moment, due to shear force, at the left and right of the effective length of the opening, as given by:

$$2M_{b,NV,Rd} + 2M_{t,NV,Rd} + M_{vc,Rd} \geq V_{Sd} l_e \quad (4)$$

where $M_{b,NV,Rd}$ is the reduced moment strength of the bottom tee for the presence of shear and axial tension, $M_{t,NV,Rd}$ is the reduced moment strength of the top tee for the presence of shear and axial tension, $M_{vc,Rd}$ is the moment strength due to local composite action between the top tee and the slab.
The V_{Sd} value is the design vertical shear force taken as the value at the lower moment side of the opening. For circular openings, the calculation method provides an equivalent rectangular opening, where its height is designated as $h_{eo} = 0.9 d_o$ and its effective length is given by $l_e = 0.45 d_o$, on which d_o is the diameter of the openings.

1.3.1.4 Longitudinal shear strength

The design longitudinal shear strength of the web post can be established as:

$$V_{wp,Rd} = \frac{0.6 s_o t_w f_y}{\gamma_{a1}} \quad (5)$$

where s_o is the edge-to-edge spacing of the openings and t_w is thickness of the web.

1.3.1.5 Bending strength of web post

The design bending strength of the web post should be calculated using the elastic strength module as follows:

$$M_{wp,Rd} = \frac{s_o^2 t_w}{6} \frac{f_y}{\gamma_{a1}} \quad (6)$$

1.3.1.6 Web post buckling

To calculate the buckling strength it is necessary to determine the reduction factor (c) as established by ABNT NBR 8800: 2008 [2]. However, the non-dimensional slenderness of the web post is given by:

$$\lambda_o = \frac{1.75\sqrt{s_o^2 + d_o^2}}{t_w \lambda_1} \quad (7)$$

where $\lambda_1 = \pi\sqrt{Ef_y}$, on which *E* and f_y are the modulus of elasticity and the yield strength of steel, respectively. The buckling resistance of the web post is given by:

$$N_{wp,Rd} = \chi \frac{s_o t_w f_y}{\gamma_{a1}} \quad (8)$$

1.3.2 Ward´s method [3]

1.3.2.1 Shear strength at an opening

The shear strength at an opening is taken equal to the shear strength of the steel section, calculated by Equation (1). Therefore, the shear strength of the concrete slab is ignored.

Figure 5 – Equivalent hexagonal castellated beam, valid for 1.08<s/d_o<1.5

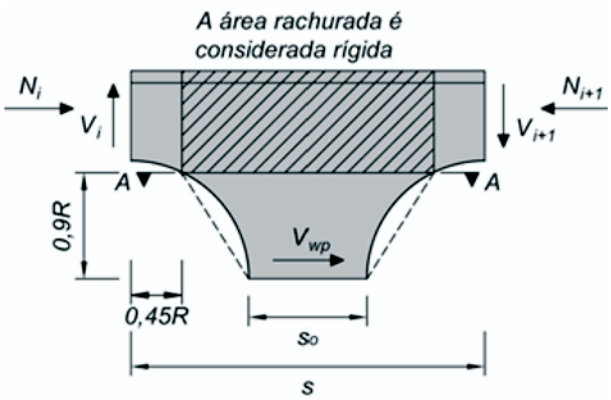

1.3.2.2 Moment strength at an opening

The moment strength of a cellular composite beam can be determined using a plastic stress distribution similar to that described in ABNT NBR 8800:2008 [2] for solid composite beams under positive bending moment and full shear connection. In case of partial shear connection, the bending resistance of the cellular composite beam is given by:

$$M_{Rd} = M_{el} + \eta_i \left(M_{pl} - M_{el}\right) \quad (9)$$

where M_{el} is the elastic moment of the steel section (both tees), η_i is the shear connection degree and M_{pl} is the plastic moment of the composite beam for full shear connection.

1.3.2.3 Vierendeel mechanism

The Vierendeel mechanism occurs due the formation of a plastic hinge at a certain angle of the circular opening, at an associated section called critical section. The interaction of secondary moments and axial forces, due to the transfer of shear and local axial force (caused by bending of the beam) through the opening is verified using the following equation:

$$\frac{N'}{N'_{Rd}} + \frac{M'}{M'_{pl}} \leq 1 \quad (10)$$

where N' e M' are forces on the critical section, N'_{Rd} is the product of the area of critical section by the yield strength of steel, f_y, and M'_{pl} is the plastic moment in the critical section for plastic sections and equal to the elastic moment for other sections.

1.3.2.4 Longitudinal shear force

The longitudinal shear resistance is calculated by Ward method [3] in the same way as shown for the Lawson and Hicks [4] method.

1.3.2.5 Web post flexural and buckling strength

The web post strength is governed by two modes of collapse: flexural failure, caused by the formation of a plastic hinge, and buckling. The failure mode depends on the web thickness and the ratio *s*/d_o (spacing of adjacent openings/diameter of openings). After a series of non-linear finite element analysis, design curves were computed for the web post, which resulted in the following verification equation:

$$\frac{M_{max}}{M_e} = \left[C_1\left(\frac{s}{d_o}\right) - C_2\left(\frac{s}{d_o}\right)^2 - C_3\right] \quad (11)$$

Figure 6 – Geometrical characteristics of the cellular composite beam from Oliveira (9) (dimensions in millimeters)

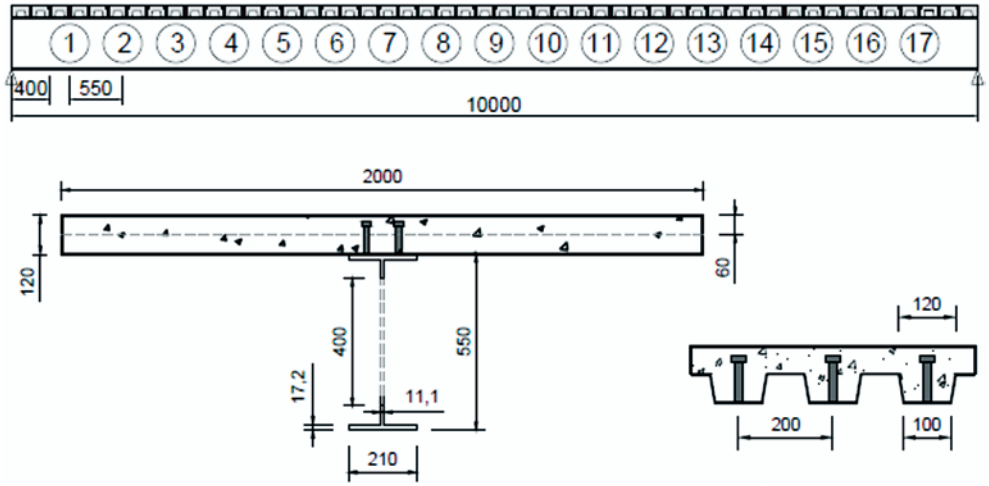

where M_{max} is the maximum allowable moment at the section A-A of Figure 5 , M_e is the elastic moment at the section A-A of Figure and C_1 , C_2 and C_3 are constants defined according to the diameter of openings and web thickness.

2. Methodology

2.1 About the program

The computer program for the design of composite cellular steel and concrete beams, called DIMCEL, was developed in MATLAB (2010) addressing the Lawson and Hicks [4] and Ward [3] methods. The program designs simply supported beams with composite steel and concrete sections composed of symmetrical cellular sections, without web stiffeners and unfilled openings. Also allows the design of steel cellular beams, i. e., without considering the contribution of the concrete slab, but considers continuous lateral restraint. Therefore, both types of construction can be analyzed: unpropped construction and propped construction. In the case of unpropped construction, just perform additional verification of the steel cellular beam subject only to construction loads.

Two types of concrete slabs are considered for the composite

Figure 7 – Geometrical characteristics of the cellular composite beam from Ward (3) (dimensions in millimeters)

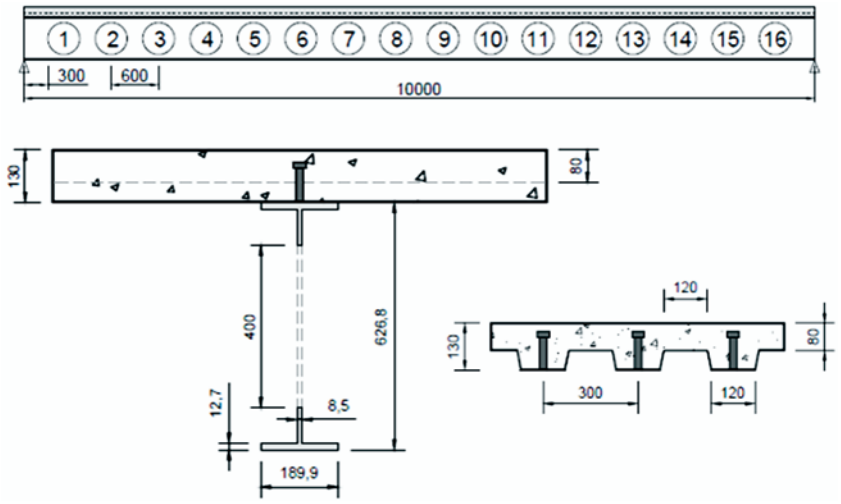

beam: solid concrete slab and composite steel and concrete slab. For shear connections, are addressed only stud shear connectors. The loads can be distributed along the length of the beam or concentrated at pre-established locations by the user.

2.2 Program validation

For the program validation, were selected two numerical examples from the literature. Oliveira´s [9] example was used to validate the method of Lawson and Hicks [4] and Ward's method [3] was validated with the example contained in his own guide.

Oliveira´s [9] example corresponds to a cellular composite steel and concrete simply supported beam. The geometrical characteristics of the composite beam are shown in Figure 6. The cellular beam was obtained from an IPE 550 section. The steel is S235. Before the concrete cure the beam self weight is 7.35 kN/m, after the cure the self weight is 7.11 kN/m, permanent load is 3 kN/m and the imposed load is 15 kN/m. The compressive strength of the concrete is 30 MPa. The beam spacing is 2 m. Stud shear connectors were used with a diameter of 19 mm and two connectors per trough.

The Ward's [3] example corresponds to a cellular composite steel and concrete simply supported beam. The geometrical characteristics of the composite beam are shown in Figure 7. The cellular beam was obtained from an UB 457x67 section. The steel is S355. Before the concrete cure the beam self weight is 2.38 kN/m², after the cure the self weight is 2.24 kN/m², the permanent load is 0.5 kN/m² and the imposed load is 6 kN/m². The compressive strength of concrete is 30 MPa. The beam spacing is 3 m. Stud shear connectors were used with a diameter of 19 mm and one connector per trough.

Table 1 compares the results of the program with the numerical example of Oliveira [9], which addresses the Lawson and Hicks [4] method and Table 2 compares the results of the program with Ward´s [3] method. The program validation was proven because it was found that the percentage differences between program results and numerical examples are due exclusively to the adopted normative criteria, since the program uses ABNT NBR 8800: 2008 while the examples have been resolved in accordance with European standards.

2.3 Experimental testing

2.3.1 Nadjai et al. [10] test

The cellular composite steel and concrete beam, denominated Ulster Beam A1, was tested by Nadjai et al. [10] and corresponds to a simply supported beam with concentrated loads applied at two points. In Figure 8, the geometric characteristics of the experimental model are presented: span between supports of 4500 mm, expanded depth equal to 575 mm, diameter of the openings equal to 375 mm and spacing of adjacent openings of 500 mm. The steel cellular beam was fabricated from an UB 406×140×39 section. The steel is S355.

The composite steel and concrete slab has a width of 1200 mm and total depth of 150 mm, in which 99 is the depth of concrete above decking profile and 51 is the overall depth of decking profile, with normal density concrete. The concrete compressive strength was evaluated by three cubic samples during the test realization, which provided an average value of 35 MPa. The slab reinforcement consisted of welded wire mesh reinforcement A142 (bars with 7 mm diameter spaced every 200 mm) with yield strength of 500 MPa.

The ultimate limit state which led the Ulster Beam A1 to failure was the web post buckling. For comparison purposes, was calculated by the program the failure load related to that limit state by both

Table 1 – Comparison of the results obtained from the Oliveira's (9) example and the computer program

	Bending at an opening (kNm)				Shear force at an opening (kN)		Vierendeel mechanism (kNm)		Longitudinal shear (kN)	
	M_{Sd}	M_{Rd}	$N_{ab,sd}$	$N_{ab,rd}$	V_{Sd}	V_{Rd}	$M_{v,Sd}$	$M_{v,Rd}$	$V_{wp,Sd}$	$V_{wp,Rd}$
Example[1]	451.86	691.51	722.03	1104.97	162.31	390.74	29.22	58.95	131.8	225.9
Program[2]	451.88	625.05	726.21	1004.52	162.31	282.47	29.22	55.11	131.81	213.42
Difference (%)	0.00	9.61	-0.58	9.09	0.00	27.71	0.00	6.51	-0.01	5.52

	Web post bending (kN)		Web post buckling (kN)		Limiting value of shear force (kN)			Deflection (mm)	
					Buckling		Bending		
	$M_{wp,Sd}$	$M_{wp,Rd}$	$N_{wp,Sd}$	$N_{wp,Rd}$	V_{Sd}	V_{Rd}	V_{Rd}		
Example[1]	0	9.78	131.8	302.97	149.11	228.38	368.58	22.33	225.9
Program[2]	0	8.89	131.81	284.56	149.12	301.61	330.93	18.2	213.42
Difference (%)	0.00	9.10	-0.01	6.08	-0.01	-32.06	10.21	18.50	5.52

[1] Oliveira's (9) example; [2] Program developed in this study.

Table 2 – Comparison of the results obtained from the Ward's (3) example and the computer program

	Bending at an opening (kNm)		Shear force at the support (kN)		Shear force at an opening (kN)		Longitudinal shear (kN)		Web post strength (kNm)	
	M_{Sd}	M_{Rd}	V_{Sd}	V_{Rd}	V_{Sd}	$V_{o,Rd}$	$V_{o,Sd}$	$V_{o,Rd}$	M_{AA}	M_{max}
Example[1]	504	808	201.6	1135	181.4	370	139	326	25	45.13
Program[2]	474.54	792.09	190.5	1031.7	171.45	373.29	131.14	329.18	23.61	41.02
Difference (%)	5.85	1.97	5.51	9.10	5.49	-0.89	5.65	-0.98	5.56	9.11

	Vierendeel mechanism $\frac{N_{IT,Sd}}{N_{I,RD}} + \frac{M_{sd}}{M_{pl}}$	Deflection (mm)
Example[1]	0.84	20.6
Program[2]	0.95	20.23
Difference (%)	-13.10	1.80

[1] Ward's (3) example; [2] Program developed in this study.

methods, Lawson and Hicks [4] and Ward [3]. From Table 3, it can be noted that both methods are safer and the method of Lawson and Hicks [4] predicted the failure load related to the limit state in question more accurately.

2.3.2 Müller et al. [11] test

The cellular composite steel and concrete beam, denominated RWTH Beam 1B, was tested by Müller et al. [11] and corresponds to a simply supported beam with a concentrated load applied at four points. In Figure 9, the geometric characteristics of the experimental model are presented: span between supports of 6840 mm, expanded depth equal to 555.2 mm, diameter of the openings equal to 380 mm and spacing of adjacent openings of 570 mm. The steel cellular beam was fabricated from an IPE 400 section. The steel is S355.

Figure 8 – Geometrical characteristics of the Ulster Beam A1 (dimensions in millimeters)

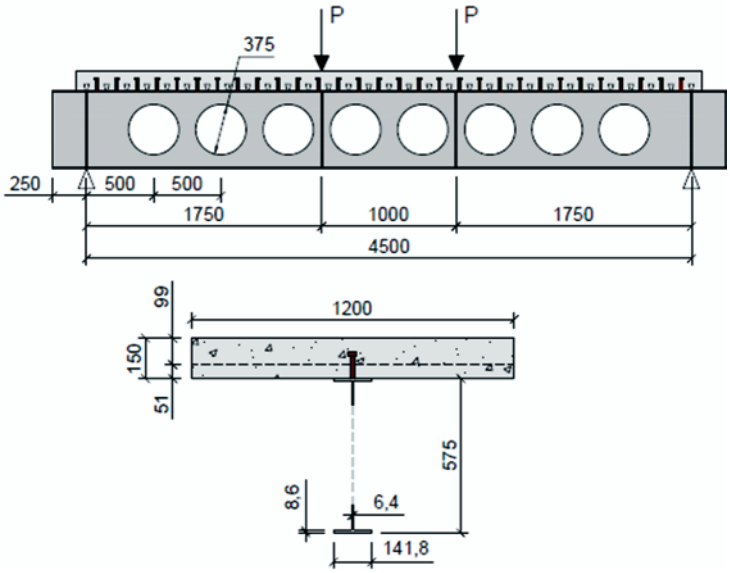

Table 3 – Comparison between the results of Nadjai et al. (10) and the program

	Failure load (kN)	Percentage difference $(P_p^* - P_e)/P_e$ x 100
Experimental (P_e)	370	–
Lawson e Hicks (4)	310	-16%
Ward (3)	276	-25%

(*) P_p = Failure load obtained by the program

Table 4 – Comparison between the results of Müller et al. (11) and the program

	Failure load (kN)	Percentage difference $(P_p^* - P_e)/P_e$ x 100
Experimental (P_e)	843.7	–
Lawson e Hicks (4)	692	-18%
Ward (3)	556	-34%

(*) P_p = Failure load obtained by the program

Müller et al. [11] considered full interaction between steel and concrete. This interaction was achieved with the use of stud shear connectors, with a diameter of 19 mm and one connector per trough. The geometric characteristics of the steel deck are the same of that shown at Ulster-A1 model.

The composite steel and concrete slab has a width of 1800 mm and total depth of 130 mm, in which 79 is the depth of concrete above decking profile and 51 is the overall depth of decking profile, with normal density concrete. In the concrete slab was used a reinforcement of 0.4% in longitudinal and transverse directions, which was located at 20 mm from top of the concrete face.

The cellular composite steel and concrete beam RWTH Beam 1B was tested with the openings 11 and 12 filled. The ultimate limit state that led the beam RWTH Beam 1B to failure was the web post buckling between the openings 1 and 2. From the calculation program results, the failure should be governed by the Vierendeel mechanism, with a load 21% lower than the experimental according to the Lawson and Hicks [4] method and a load 42% lower than the experimental according to the Ward´s [3] method.

The Table 4 shows the comparison between the experimental results and computational program for each method considering the web post buckling that governed the experimental failure. It may be noted that both methods are safer and the method of Lawson and Hicks [4] was more accurate in the prediction of the failure load related to the limit state in question.

3. Results and discussions

The parametric study of cellular composite beams was performed considering beams obtained from two I rolled section, W 310x32.7 and W 530x85. The study was realized to simply supported beams subjected to a uniformly distributed load, considering propped construction. The steel is ASTM A572 (Grade 50).

The slab studied is composite steel and concrete with overall depth of decking profile equal to 75 mm, parallel to the beam span and composed of concrete with compressive strength of 30 MPa. The total height of the slab was 130 mm and the beam spacing was 3 m.

Figure 9 – Geometrical characteristics of the RWTH Beam 1B (dimensions in millimeters)

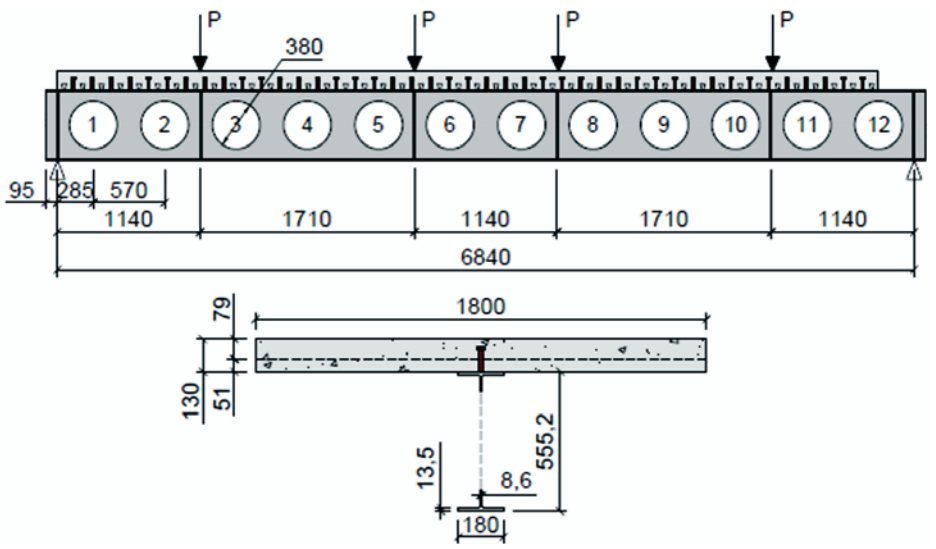

Table 5 – Geometric parameters adopted for the W 310x32.7 section

d	d_o	S	$L_{/dg}$
$1.3d_g$	0.6d	$1.3d_o$, $1.4d_o$ and $1.5d_o$	10, 15, 20, 25, 30, 35 and 40
	0.7d	$1.3d_o$, $1.4d_o$ and $1.5d_o$	10, 15, 20, 25, 30, 35 and 40
	0.8d	$1.3d_o$, $1.4d_o$ and $1.5d_o$	10, 15, 20, 25, 30, 35 and 40
$1.4d_g$	0.63d	$1.3d_o$	10, 15, 20, 25, 30, 35 and 40
	0.7d	$1.3d_o$, $1.4d_o$ and $1.5d_o$	10, 15, 20, 25, 30, 35 and 40
	0.8d	$1.3d_o$, $1.4d_o$ and $1.5d_o$	10, 15, 20, 25, 30, 35 and 40
$1.5d_g$	0.73d	$1.3d_o$	10, 15, 20, 25, 30, 35 and 40
	0.8d	$1.3d_o$, $1.4d_o$ and $1.5d_o$	10, 15, 20, 25, 30, 35 and 40
$1.57d_g$	0.8d	$1.3d_o$	10, 15, 20, 25, 30, 35 and 40

Stud shear connectors with 19 mm diameter were adopted. Initially, the number of connectors was calculated considering full interaction between steel and concrete for the solid composite beams that originated the studied cellular composite beams. The same number of shear connectors was adopted to the cellular composite beams.

The Ward [3] and Lawson and Hicks [4] methods have different geometric limits for cellular beams. In this study, the geometric parameters of the beams have been defined according to the limits of both methods. Tables 5 and 6 show respectively the parameters and the ratio L/d_g (span length/expanded depth) adopted for the sections W 310x32.7 and W 530x85. The depth of the original solid beam was designated as d_g, the diameter of the opening as d_o and the spacing of adjacent openings as s. Initially, the composite beams were calculated with the original solid steel section, to determine its ultimate load (P_{VM}) and the limit state associated with the failure. Then, the program here developed was used for the calculation of cellular composite beams and obtaining the ultimate load (P_{VC}). Thus, the percentage difference between the ultimate load of the cellular composite beam and the solid composite beam can be calculated as:

$$\delta = \left(P_{VC} - P_{VM}\right) / P_{VM} \times 100\,(\%) \qquad (12)$$

If the percentage difference is less than zero, it means that the solid composite beam resists better to the applied load than the cellular composite beam, otherwise the cellular composite beam performs better.

To determine the ultimate load for the solid and cellular beams, a routine was developed in the computer program which is able to increase the load value until it reaches the beam failure load, and then writing the value of the failure load and the failure mode in a spreadsheet. The verification of the ultimate limit states was realized considering all applied loads (permanent and imposed loads) multiplied by 1.4. To verify the serviceability limit state of excessive deflection, it was considered that 40% of the total load was permanent and, therefore, was used this portion of loading to calculate the long-term deflection. The imposed load was taken as 60% of the total load, for the determination of its short-term deflection.

Table 6 – Geometric parameters adopted for the W 530x85 section

d	d_o	S	$L_{/dg}$
$1.3d_g$	0.6d	$1.3d_o$, $1.4d_o$ and $1.5d_o$	10, 15, 20, 25, 30, 35 and 40
	0.7d	$1.3d_o$, $1.4d_o$ and $1.5d_o$	10, 15, 20, 25, 30, 35 and 40
	0.8d	$1.3d_o$, $1.4d_o$ and $1.5d_o$	10, 15, 20, 25, 30, 35 and 40
$1.4d_g$	0.63d	$1.3d_o$	10, 15, 20, 25, 30, 35 and 40
	0.7d	$1.3d_o$, $1.4d_o$ and $1.5d_o$	10, 15, 20, 25, 30, 35 and 40
	0.8d	$1.3d_o$, $1.4d_o$ and $1.5d_o$	10, 15, 20, 25, 30, 35 and 40
$1.5d_g$	0.73d	$1.3d_o$	10, 15, 20, 25, 30, 35 and 40
	0.8d	$1.3d_o$, $1.4d_o$ and $1.5d_o$	10, 15, 20, 25, 30, 35 and 40
$1.57d_g$	0.8d	$1.3d_o$	10, 15, 20, 25, 30, 35 and 40

Table 7 – Limit state and ultimate load for the solid composite beams

	W 310x32.1		W 530x85	
L/d_g	q_{max} (kN/m)	Limit state	q_{max} (kN/m)	Limit state
10	168.3	Yielding due to bending	208.65	Yielding due to bending
15	85.7	Yielding due to bending	98.7	Excessive deflection
20	43.3	Excessive deflection	45.4	Excessive deflection
25	23.55	Excessive deflection	24.1	Excessive deflection
30	14.25	Excessive deflection	13.95	Excessive deflection
35	9.3	Excessive deflection	8.8	Excessive deflection
40	6.4	Excessive deflection	5.9	Excessive deflection

3.1 Solid composite beam designed by ABNT NBR 8800:2008

Table 7 shows the limit state that governs the design of the solid composite beams for each ratio L/d_g (beam span/depth of the solid beam) and their associated ultimate loads.

3.2 Cellular composite beam designed by the Lawson and Hicks [4] method

In the parametric study, the symbols for identification of the cellular composite beams were given by the designation: VC d_g - d/d_g - d_o/d - s/d_o - L/d_g, where VC indicates cellular composite beam and the variables d_g, d , d_o, s and L are the geometric parameters. For example, VC 310-1.3-0.6-1.3-10 means a cellular composite beam with 310 mm of depth of the original solid section, d_g, the ratio between the expanded depth and the depth of the original section, d/d_g equal to 1.3, the ratio between the diameter of the opening and the expanded depth, d_o/d equal to 0.6, the ratio between the spacing of adjacent openings and the diameter of the opening, s/d_o, equal to 1.3 and the ratio between the beam span and depth of the original solid section equal to 10.

Table 8 shows the cellular composite beams obtained from a W 310x32.7 section that presented the best performance (higher resistance or lower deflection, depending on the governing limit state) in relation to the solid composite beam. The limit state that governed the design is mentioned in the table.

At Table 8, it can be noted that the use of cellular composite beams obtained from the W 310x32.7 section is advantageous for L/d_g ratio equal or greater than 25, when the limit state of the solid composite beam is governed by the excessive deflection and, thus, the services stresses are relatively low. It can also be noticed that the most adequate geometry for the cellular composite beams in this case is that with expanded depth equal to 1.5 times the depth of the original section, diameter of openings equal to 0.73 times the expanded depth and spacing of adjacent openings equal to 1.3 times the diameter of the openings.

Table 9 shows the cellular composite beams obtained from a W 530x85 section that presented the best performance in relation to the solid composite beam. The limit state that governed the design is mentioned in the table.

At Table 9, it can be noted that the use of cellular composite beams obtained from a W 530x85 section is advantageous for L/d_g ratio equal or greater than 20. It can also be noticed that the most adequate geometry for the cellular composite beams in this case is that with expanded depth equal to 1.5 times the depth of the

Table 8 – Ultimate load and associated limit state for cellular composite beams obtained from a W 310x32.7 section

L/d_g	δ(*)	Designation	Limit state
10	-29%	VC 310-1.3-0.6-1.5-10	Vierendeel mechanism
15	-20%	VC 310-1.3-0.6-1.5-15	Yielding due to bending
20	-8%	VC 310-1.5-0.73-1.3-20	Web post buckling
25	13%	VC 310-1.5-0.73-1.3-25	Yielding due to bending
30	32%	VC 310-1.5-0.73-1.3-30	Yielding due to bending
35	48%	VC 310-1.5-0.73-1.3-35	Yielding due to bending
40	66%	VC 310-1.5-0.73-1.3-40	Yielding due to bending

(*) Percentage difference

Table 9 – Ultimate load and associated limit state for cellular composite beams obtained from a W 530x85 section

L/d_g	δ(*)	Designation	Limit state
10	-19%	VC 530-1.3-0.6-1.5-10	Vierendeel mechanism
15	-8%	VC 530-1.3-0.6-1.5-15	Yielding due to bending
20	20%	VC 530-1.4-0.63-1.3-20	Yielding due to longitudinal shear
25	52%	VC 530-1.5-0.73-1.3-25	Yielding due to bending
30	82%	VC 530-1.6-0.8-1.3-30	Web post buckling
35	105%	VC 530-1.6-0.8-1.3-35	Excessive deflection
40	103%	VC 530-1.6-0.8-1.3-40	Excessive deflection
(*) Percentage difference			

original section, diameter of openings equal to 0.73 times the expanded depth and spacing of adjacent openings equal to 1.3 times the diameter of the openings.

The analysis of the Tables 8 and 9 also shows a greater economic advantage in the use of cellular composite beams with greater depth, since the percentage difference between the ultimate load of the cellular composite beam and the solid cellular beam, d, is greater for W 530x85 section for all L/d_g ratios. Also, it is noted that the higher the L/d_g ratio, the greater the percentage difference, reaching more than 100% for the VC 530-1.6-0.8-1.3-35 and VC 530-1.6-0.8-1.3-40 beams, i.e., these beams have more than the double of the ultimate load of its corresponding solid-composite beams for the L/d_g ratios equal to 35 and 40.

Table 10 shows the relation between the geometry of the cellular composite beam obtained from a W 310x32.7 section and the failure modes. It can be noted that yielding due to longitudinal shear occurs in small to medium spans (L/d_g equal to 10, 15 and 20) in beams with a small width of the web post, or in cases where the s/d_o ratio is less than 1.4 and the d_o/d_g ratio is less than 0.63. The Vierendeel mechanism governed the design in cases of small to medium spans (L/d_g equal to 10, 15 and 20), and the d_o/d_g ratio equal to 0.8, that is, when the width of the web post was larger. For medium spans (L/d_g equal to 20 and 25), the web post buckling was predominant only for higher values of the expanded depth, i.e., d/d_g ratio equal to 1.5 to 1.57. For large spans (L/d_g equal to 30, 35 and 40), the critical limit states were yielding due to bending and excessive deflection. However, the excessive deflection did not occur for L/d_g ratio equal to 30.

Table 11 shows the relation between the geometry of the cellular composite beam obtained from a W 530x85 section and the fail-

Table 10 – Relation between the geometry of the cellular composite beam obtained from a W 310x32.7 section and the failure modes

Designation	Limit state
Yielding due to longitudinal shear	$L/d_g \leq 15$, $d_o \leq 0.63d$ and $s \leq 1.4d_o$
	$L/d_g \leq 15$, $d_o = 0.7d$ and $s = 1.3d_o$
	$L/d_g = 20$, $d_o \leq 0.63\ d_o$ and $s = 1.3d_o$
Web post buckling	$15 \leq L/d_g \leq 20$, $d = 1.5d_g$ and $d_o = 0.73d$
	$20 \leq L/d_g \leq 25$ and $d = 1.57d_g$
Vierendeel mechanism	$L/d_g \leq 15$ and $d_o \geq 0.7d$, except in cases where occurred longitudinal shear
	$L/d_g = 20$ and $d_o = 0.8d$
Excessive deflection	$L/d_g = 40$ and $d = 1.3d_g$
	$L/d_g = 40$, $d = 1.4d_g$ and $s \leq 1.4d_o$
	$L/d_g = 35$, $d = 1.3d_g$ and $d_o = 0.6d$
	$L/d_g = 35$, $d = 1.3d_g$, $d_o = 0.7d$ and $s = 1.3d_o$
Yielding due to bending	$L/d_g \geq 25$ except in cases where occurred excessive deflection
	$L/d_g = 20$ and $d_o \leq 0.7d$, except in cases where occurred longitudinal shear
	$L/d_g = 15$, $d_o = 0.6d$ and $s = 1.5d_o$

Table 11 – Relation between the geometry of the cellular composite beam obtained from a W 530x85 section and the failure modes

Limit state	Geometric parameters
Yielding due to longitudinal shear	$L/d_g \leq 15$, $d_o \leq 0.63d$ and $s \leq 1.4d_o$
	$L/d_g = 15$, $d_o = 0.7d$ and $s = 1.3d_o$
	$L/d_g = 20$, $d_o \leq 0.63d$ and $s = 1.3d_o$
Web post buckling	$L/d_g \leq 20$, $d = 1.4d_g$, $d_o = 0.7d$ and $s = 1.3d_o$
	$L/d_g \leq 20$, $d = 1.5d_g$ and $d_o = 0.73d$
	$20 \leq L/d_g \leq 25$, $d = 1.5d_g$, $d_o = 0.8d$ and $s = 1.3d_o$
	$20 \leq L/d_g \leq 25$ and $d = 1.6d_g$
Vierendeel mechanism	$L/d_g \leq 15$ and $d_o \geq 0.7d$, except in cases where occurred longitudinal shear
	$L/d_g = 20$ and $d_o = 0.8d$
Yielding due to bending	$L/d_g = 15$, $d = 1.3dg$, $d_o = 0.6d$ and $s = 1.5d_o$
	$L/d_g = 20$, $d_o \leq 0.7d$ and $s \geq 1.4d_o$
	$L/d_g = 25$ and $d_o \geq 0.7d$
	$L/d_g = 30$, $d = 1.4d_g$, $d_o = 0.8d$ and $s = 1.5d_o$
	$L/d_g = 30$, $d = 1.5d_g$ and $d_o = 0.8d$
Excessive deflection	$L/d_g >= 35$
	$L/d_g = 30$ and $d_o \leq 0.73d$
	$L/d_g = 30$, $d_o = 0.8d$ and $d \leq 1.4d_g$
	$L/d_g = 25$ and $d_o \leq 0.63d$

ure modes. It can be noted that yielding due to longitudinal shear occurs in small to medium spans (L/d_g equal to 10, 15 and 20) in beams with a small width of the web post, or in cases where the s/d_o ratio is less than 1.4 and the d_o/d_g ratio is less than 0.63. The Vierendeel mechanism governed the design in cases of small to medium spans (L/d_g equal to 10, 15 and 20), and the d_o/d_g ratio equal to 0.8, that is, when the width of the web post was larger. The web post buckling occurs in small to large spans (L/d_g equal to 10, 15, 20, 25 and 30), principally in beams with larger values of expanded depth, ie, d/d_g ratio greater than or equal 1.5. Yielding due to bending governed the design, mainly, in medium spans (L/d_g equal to 25), in beams with lower values of expanded depth, i.e., d/d_g ratio less than 1.5, and d_o/d ratio greater than 0.63. For large spans (L/d_g equal to 35 and 40) the limit state of excessive deflection always governed the design.

3.3 Cellular composite beam design by Ward´s [3] method

Table 12 shows the cellular composite beams obtained from a W

Table 12 – Ultimate load and associated limit state for cellular composite beams obtained from a W 310x32.7 section

L/d_g	$\delta^{(*)}$	Designation	Limit state
10	-42%	VC 310-1.3-0.6-1.5-10	Vierendeel mechanism
15	-28%	VC 310-1.3-0.6-1.5-15	Vierendeel mechanism
20	-12%	VC 310-1.3-0.6-1.5-20	Vierendeel mechanism
25	7%	VC 310-1.5-0.73-1.3-25	Web post bending and buckling
30	20%	VC 310-1.5-0.73-1.3-30	Excessive deflection
35	20%	VC 310-1.57-0.8-1.3-35	Excessive deflection
40	19%	VC 310-1.57-0.8-1.3-35	Excessive deflection

(*) Percentage difference

Table 13 – Ultimate load and associated limit state for cellular composite beams obtained from a W 530x85 section

L/d_g	δ(*)	Designation	Limit state
10	-41%	VC 530-1.3-0.6-1.5-10	Web post bending and buckling
15	-8%	VC 530-1.3-0.6-1.5-15	Vierendeel mechanism
20	17%	VC 530-1.3-0.6-1.5-20	Excessive deflection
25	41%	VC 530-1.5-0.73-1.3-25	Excessive deflection
30	52%	VC 530-1.6-0.8-1.3-30	Excessive deflection
35	52%	VC 530-1.6-0.8-1.3-35	Excessive deflection
40	53%	VC 530-1.6-0.8-1.3-40	Excessive deflection
(*) Percentage difference			

310x32.7 section that showed the best performance in relation to the solid composite beam. The limit state that governed the design is mentioned in the table.

At Table 12, it can be noted that the use of cellular composite beams obtained from a W 310x32.7 section is advantageous for L/d_g ratio equal or greater than 25. It can also be noticed that the most adequate geometry for the cellular composite beams in this case is that with expanded depth equal to 1.5 or 1.57 times the depth of the original section, diameter of openings ranging from 0.73 to 0.8 times the expanded depth and spacing of adjacent openings equal to 1.3 times the diameter of the openings.

Table 13 shows the cellular composite beams obtained from a W 530x85 section that showed the best performance in relation to the solid composite beams. The limit state that governed the design is mentioned in the table.

At Table 13, it can be noted that the use of cellular composite beams obtained from a W 530x85 section is advantageous for L/d_g ratio equal or greater than 20. It can also be noticed that the most adequate geometry for the cellular composite beams in this case is that with expanded depth ranging from 1.3 to 1.5 times the depth of the original section, diameter of openings ranging from 0.6 to 0.8 times the expanded depth and spacing of adjacent openings ranging from 1.3 to 1.5 times the diameter of the openings.

The analysis of Tables 12 and 13 also shows a greater economic advantage in the use of cellular composite beams with greater depth, since the percentage difference between the ultimate load of cellular composite beam and the solid cellular beam, d, is greater for the W 530x85 section for all L/d_g ratios. Also, it is noted that the higher the L/d_g ratio, the greater the percentage difference, reaching more than 50% for the VC 530-1.6-0.8-1.3-35 and VC 530-1.6-0.8-1.3-40 beams.

Table 14 shows the relation between the geometry of the cellular composite beam obtained from a W 310x32.7 section and the failure modes. It can be noted that the web post bending and buckling occurs in small to medium spans (L/d_g equal to 10, 15, 20 and 25) in beams with a small width of the web post, or in cases where the

Table 14 – Relation between the geometry of the cellular composite beam obtained from a W 310x32.7 section and the failure modes

Limit state	Geometric parameters
Web post bending and buckling	$L/d_g \leq 20$, $d_o \leq 0.7d$ and $s=1.3d_o$
	$L/d_g \leq 20$, $d_o=0.6d$ and $s=1.4d_o$
	$L/d_g \leq 25$, $d_o \leq 0.73d$ and $s=1.3d_o$
Vierendeel mechanism	$L/d_g \leq 25$ and $d_o=0.8d$
	$L/d_g \leq 20$, $d_o=0.7$ and $s \geq 1.4d_o$
	$L/d_g =30$, $d_o=0.8$ and $d \geq 1.4d_o$
Excessive deflection	$L/d_g =25$, $d=1.3d_g$, $d_o \leq 0.7d$ and $s \geq 1.4d_o$
	$L/d_g =25$, $d=1.3d_g$, $d_o=0.7d$ and $s=1.3d_o$
	$L/d_g =25$, $d=1.4d_g$, $d_o=0.7d$ and $s=1.4d_o$
	$L/d_g =30$ and $d_o \leq 0.73d$
	$L/d_g =30$, $d_o=0.8d$ and $d=1.3d_g$
	$L/d_g \geq 35$

Table 15 – Relation between the geometry of the cellular composite beam obtained from a W 530x85 section and the failure modes

Limit state	Geometric parameters
Web post bending and buckling	$L/d_g \leq 20$, $d_o \leq 0.7d$ and $s=1.3d_o$
	$L/d_g \leq 20$, $d_o=0.6d$ and $s=1.4d_o$
	$L/d_g=10$, $d_o=0.6d$ and $s=1.5d_o$
Vierendeel mechanism	$L/d_g \leq 25$ and $d_o=0.8d$
	$L/d_g \leq 20$, $d_o=0.7$ and $s \geq 1.4d_o$
Excessive deflection	$L/d_g=20$, $d_o=0.6d$ and $s=1.5d_o$
	$L/d_g=25$ and $d_o \leq 0.7d$
	$L/d_g \geq 30$

s/d_o ratio is less than 1.4 and the d_o/d_g ratio is less than 0.63. The Vierendeel mechanism governed the design in cases of small to large spans (L/d_g equal to 10, 15, 20, 25 e 30), and the d_o/d_g ratio equal to 0.8, that is, when the width of the web post was larger. For large spans (L/d_g equal to 30, 35 and 40), the critical limit states was the excessive deflection.

Table 15 shows the relation between the geometry of the cellular composite beam obtained from a W 530x85 section and the failure modes. It can be noted that the web post bending and buckling occurs in small to medium spans (L/d_g equal to 10, 15 and 20) in beams with a small width of the web post, or in cases where the s/d_o ratio is less than 1.4 and the d_o/d_g ratio is less than 0.73. The Vierendeel mechanism governed the design in cases of small to large spans (L/d_g equal to 10, 15, 20, 25 e 30), and the d_o/d_g ratio equal to 0.8, that is, when the width of the web post was larger. For large spans (L/d_g equal to 30, 35 and 40), the critical limit states was the excessive deflection.

3.4 Methods comparison

Figure 10 shows the comparison between the best performance ultimate load of the cellular composite beams obtained by both methods (higher strength or lower deflection, depending on the limit state that governs the design) in relation to the solid composite beams. The analysis of Figure 10 shows that in most cases studied Ward´s [3] method shows more conservative results.

4. Conclusions

Two methods for the design of cellular composite beams were

Figure 10 – Comparison between the ultimate load of the cellular composite beams obtained by Ward (3) and Lawson and Hicks (4) methods

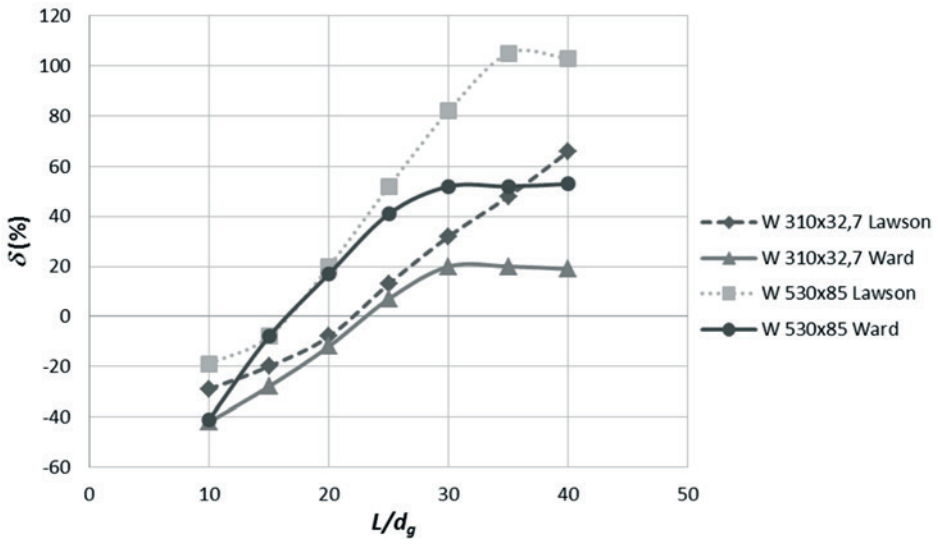

studied: Ward´s [3] and Lawson and Hicks [4] methods. Both methods use prescriptions of European standards when it comes to limit states and design strengths already established. In this work, an adaptation of the methods to conform with ABNT NBR 8800: 2008 [2] was carried out.

A computer program for the design of cellular composite steel and concrete beams addressing both cited methods was developed in MATLAB (2010). The validation of the computer program was realized using two numerical examples available in the literature.

After the program validation, the adequacy of the methodologies has been verified by experimental testing, comparing the results of the computer program with results of experimental tests available in the literature, namely, the results of Nadjai et al. [10] and Müller et al. [11]. It was observed that both Lawson and Hicks [4] and Ward´s [3] methods showed slightly conservative results, however the Lawson and Hicks [4] method was more accurate in the prediction of the failure load.

Finally, a parametric study of cellular composite beams obtained from two laminated sections was conducted, W 310x32.7 and W 530x85. The study was realized for both methods presented, from which it was possible to obtain a number of conclusions about the calculation procedures:

- Both methods showed that the use of cellular composite beams is advantageous when the L/d ratio is greater or equal to 20. This was expected, since in these cases, what governs design of solid composite beams is excessive deflection and the cellular beams present higher moment of inertia. It is worth noting that, in practice, the composite beams are used to achieve larger spans $L/d \geq 25$;
- Both methods showed a greater economic advantage in the use of cellular composite beams of greater depth, as the percentage difference between the ultimate load of the cellular composite beam and the solid composite beam, d, was higher for the W 530x85 profile for all L/d ratios;
- The procedures proposed by Ward [3] for the verification of the web post buckling and bending, Vierendeel mechanism and excessive deflection generated more conservative results, which made the Lawson and Hicks [4] method provide ultimate loads higher in all analyzed cases.

5. Acknowledgements

The authors would like to thank the institutions CNPq, CAPES, FAPES and PPGEC/UFES for their support in the realization of this research.

6. References

[1] PINHO, F. O. Vigas casteladas e celulares. Estruturas metálicas com mais resistência, menos deformação e redução de peso. www.arcorweb.com.br. 2009.

[2] ASSOCIAÇÃO BRASILEIRA DE NORMAS TÉCNICAS. NBR 8800: Projeto de estruturas de aço e de estruturas mistas de aço e concreto de edifícios. Rio de Janeiro, 2008.

[3] WARD, J. K. Design of composite and non-composite cellular beams, The Steel Construction Institute, 1990.

[4] LAWSON, R. M.; HICKS, S. J. P355: Design of composite beams with large web openings: in accordance with Eurocodes and the UK National Annexes. Steel Construction Institute, 2011.

[5] TSAVDARIDIS, K.D.; D'MELLO, C. Behavior and Strength of Perforated Steel Beams with Novel Web Opening Shapes. Journal of Constructional Steel Research, v. 67, p. 1605-1620, 2011.

[6] KERDAL, D.; NETHERCOT D.A. Failure modes for castellated beams. Journal of Constructional Steel Research, p. 295-315, 1984.

[7] SILVEIRA, E. G. Avaliação do comportamento estrutural de vigas alveolares de aço com ênfase nos modos de colapso por plastificação. Dissertação de Mestrado, Viçosa: UFV, 2011

[8] ASSOCIAÇÃO BRASILEIRA DE NORMAS TÉCNICAS. NBR 6118: Projeto de estruturas de concreto - Procedimento. Rio de Janeiro, 2014.

[9] OLIVEIRA, T. C. P. Vigas alveoladas: metodologias de dimensionamento. Dissertação de Mestrado, Universidade de Aveiro, 2012.

[10] NADJAI, A.; VASSART, O.; ALI, F.; TALAMONA, D.; ALLAM, A.; HAWES, M. Performance of cellular composite floor beams at elevated temperatures, Fire Safety Journal, v. 42, p. 489-497, 2007.

[11] MÜLLER, C.; HECHLER, O.; BUREAU, A.; BITAR, D.; JOYEUX, D.; CAJOT, L. G.; DEMARCO, T.; LAWSON, R. M.; HICKS, S.; DEVINE, P.; LAGERQVIST, O.; HEDMAN-PÉTURSSON, E.; UNOSSON, E.; FELDMANN, M. Large web openings for service integration in composite floors. Technical steel research, 2006.